

FTUV-11-2705

# Top quark tensor couplings

**Gabriel A. González-Sprinberg<sup>1\*</sup>, Roberto Martínez<sup>2†</sup>, Jorge Vidal<sup>3‡</sup>**

<sup>1</sup>Instituto de Física, Facultad de Ciencias, Universidad de la República, Iguá 4225, Montevideo 11600, Uruguay.

<sup>2</sup> Departamento de Física, Universidad Nacional de Colombia, Bogotá, Colombia.

<sup>3</sup> Departament de Física Teòrica Universitat de València, E-46100 Burjassot, València, Spain and IFIC, Centre Mixt Universitat de València-CSIC, València, Spain.

## Abstract

We compute the real and imaginary parts of the one-loop electroweak contributions to the left and right tensorial anomalous couplings of the  $tbW$  vertex in the Standard Model (SM). For both tensorial couplings we find that the real part of the electroweak SM correction is close to 10% of the leading contribution given by the QCD gluon exchange. We also find that the electroweak real and imaginary parts for the anomalous right coupling are almost of the same order of magnitude. The one loop SM prediction for the real part of the left coupling is close to the  $3\sigma$  discovery limit derived from  $b \rightarrow s\gamma$ . Besides, taking into account that the predictions of new physics interactions are also at the level of a few percents when compared with the one loop QCD gluon exchange, these electroweak corrections should be taken into account in order to disentangle new physics effects from the standard ones. These anomalous tensorial couplings of the top quark will be investigated at the LHC in the near future where sensitivity to these contributions may be achieved.

---

\*Email: [gabrielg@fisica.edu.uy](mailto:gabrielg@fisica.edu.uy)

†Email: [remartinezm@unal.edu.co](mailto:remartinezm@unal.edu.co)

‡Email: [vidal@uv.es](mailto:vidal@uv.es)

# 1 Introduction

Top quark physics at the Large Hadron Collider (LHC) is an important scenario for testing physics above the electroweak scale. No deviation from the predictions of the Standard Model (SM) is found in top data [1], nowadays dominated by the Tevatron experiments. This situation may change with the LHC already running and taking data. The SM dominant decay mode  $t \rightarrow bW^+$  will be precisely measured at the LHC and sensitivity beyond tree level SM will be achieved. It is generally believed that, due to its large mass, physics of the top quark will be useful to probe new theories above the electroweak scale [2, 3]. At the LHC, top new physics may show up in new top quark decay channels or in the measurement of the top standard and anomalous couplings [3, 4]. In renormalizable theories, the anomalous couplings appear as quantum corrections, as it is the case for the SM, and also in many new physics theories. In a model independent approach there are two ways of parameterize the unknown physics at high scales. One is the effective Lagrangian method [5] which is a way to describe low energy physics effects originated at a higher energy scale. These effects are parameterized with non-renormalized terms invariant under the SM gauge symmetry  $SU(3)_c \times SU(2)_L \times U(1)_Y$  and written in terms of the low energy (standard) particle spectrum fields. It is assumed that the new particles spectrum lies at an energy scale well above the electroweak scale. The other way is just by assuming the most general form of the Lorentz structure for the  $tbW$  amplitude. There are many terms in the effective Lagrangian that may give contributions to the same Lorentz structure in the vertex, in particular to the tensorial couplings we are interested in. Besides, some of those terms can be rewritten by using the equations of motion, so the identification of the effective Lagrangian terms with the form factors is not direct nor unique. In this paper we will use the second approach, parameterizing in the most general way the  $tbW$  amplitude. This approach has the advantage, over the effective Lagrangian approach, that it does not break down even if any relatively light particles, as new scalars, for example, come into the game.

Some effects related to the top anomalous couplings, both in the  $t \rightarrow bW^+$  polarized branching fractions –for the three helicity W possibilities– and in single top production at the Tevatron and at the LHC, have already been studied in the recent years [3, 6]. However, at the LHC it will be possible to have new suitable observables in order to perform precise measurements of the anomalous couplings. Some aspect of this top quark physics have also been investigated in models with an extended Higgs sector, technicolor models, supersymmetry models and Little Higgs models [7].

The anomalous couplings are gauge invariant quantities so one can think of testing the SM predictions and new theories through observables that are directly sensitive to them. In fact,

not only top branching fractions and cross sections are predictions of the models to be confronted with data but, in the same way as in the past the anomalous magnetic moment for the electron gave the first success of quantum field theory, also these  $tbW$  gauge invariant tensorial couplings can be used to check the predictions of new physics theories. One loop QCD and electroweak contributions to the top branching fractions for polarized  $W$ 's have been studied in the frame of the SM [8]. These contributions, and the corresponding measurements, have no special sensitivity to the anomalous couplings which enter in the observables as small corrections. The explicit dependence of the polarized branching fractions on the anomalous couplings have been computed in [9, 10], where also the sensitivity to them has been considered. Specific observables that are directly proportional to the tensorial couplings have been studied in [6, 10–12] and more recently new observables were presented in [13].

In this paper we compute the electroweak SM contribution to the left and right “magnetic” tensorial couplings of the  $tbW$  vertex and we discuss their observable effects; we also compare this contributions with some new physics predictions considered in the literature. These CP-conserving pieces of the  $tbW$  vertex are different from zero only at one loop in the SM and the same is true in many extended models. The QCD gluon-exchange contribution to the tensorial couplings is the dominant one and has been reported in the literature only for the right coupling [14, 15]. The left tensorial coupling is proportional to the bottom quark-mass due to the chirality flipping property of this coupling and by the fact that it only couples to a right b-quark. For these reasons it is suppressed and it is generally assumed to be negligible. However, the measurement of both of them appears as feasible in dedicated observables computed for top production at the LHC.

For the right tensorial  $tbW$  coupling the comparison with the SM is usually performed in the literature by taking as a reference only the one loop QCD contribution. The most promising new physics models predict a few percents deviation from this QCD-value. However, as it is shown in this paper, we found that the electroweak contribution is also at the level of 10% with respect to the leading gluon exchange, and should be taken into account when comparing with data. Detailed studies will be necessary in order to disentangle new physics contributions from the electroweak standard ones.

In section 2 we define the anomalous couplings and we review the theoretical as well as the experimental status for the physics for which they are involved. In section 3 our computation is presented and in the final section we present our conclusions.

## 2 The tensorial $tbW$ vertex: experiment, SM and beyond

For on-shell particles, the most general amplitude  $\mathcal{M}_{tbW}$  for the decay  $t(p) \rightarrow b(k)W^+(q)$  can be written in the following way:

$$\mathcal{M}_{tbW^+} = -\frac{e}{\sin\theta_W\sqrt{2}} \varepsilon^{\mu*} \bar{u}_b \left[ \gamma_\mu (V_L P_L + V_R P_R) + \frac{i\sigma_{\mu\nu} q^\nu}{m_W} (g_L P_L + g_R P_R) \right] u_t, \quad (1)$$

with  $P_{L,R} = (1 \mp \gamma_5)/2$ ;  $p$ ,  $k$  and  $q = p - k$  denote the top, bottom and  $W$  boson four momenta, respectively. The tensorial left and right magnetic moments are  $g_L$  and  $g_R$  respectively. The tree level SM couplings are  $V_R = 0$ ,  $V_L = V_{tb}$  (the Cabibbo-Kobayashi-Maskawa, CKM, matrix element),  $g_R = 0$  and  $g_L = 0$ . This expression for the amplitude, written in terms of the most general form factors, is appropriate for a model independent analysis of the  $tbW$  amplitude. The anomalous form factors  $g_R$  and  $g_L$  are chirality flipping and dimensionless functions of  $q^2$ . For all particles on-shell, as can be assumed for the top decay, we have  $q^2 = M_W^2$ . Besides, these dipole moments are gauge independent quantities and may be measured with appropriate observables.

These form factors are generated by quantum corrections in the SM. In renormalizable theories, such as some extensions of the SM,  $V_R$  can appear at tree-level while tensor couplings  $g_R$  and  $g_L$ , are induced as one loop quantum corrections. Values of  $|V_L|$  different from the ones given by the global fit [16] in the SM  $V_{tb} \simeq 1$ , that we assume, are not experimentally excluded [17] and they are still an open window to test new physics. This issue (and also possible deviations of  $V_R = 0$ ) will not be the object of our work, where we concentrate only on  $g_R$  and  $g_L$ .

In renormalizable theories, the tensorial couplings are finite quantum corrections quantities that do not receive contributions from renormalization counter-terms at one loop. In addition, contrary to what happens for the  $V_R$  form factor, the tensors  $g_{L,R}$  couplings are infrared safe quantities. One loop QCD corrections generate the leading contribution to the tensorial couplings  $g_R$  and  $g_L$ . This one loop QCD gluon exchange contribution to  $g_R$  was computed in [15] and they found the value  $g_R^{QCD} = -6.61 \times 10^{-3}$ . Direct observables with sensitivity to  $g_R$  will be accessible to the LHC experiments as was discussed in [11]. The left tensorial coupling term couples a right b-quark and thus it is proportional to  $m_b$ . For this reason, it is generally believed that the SM value for  $g_L$  is much smaller than the one for  $g_R$ . We will show that this is not exactly the case.

New physics signals can also show up in the analysis of the top decay  $t \rightarrow bW^+$ . In particular, significant deviations from the SM predictions for  $g_R$  and  $g_L$  may be found. However, the SM values are only known for  $g_R$  up to one loop in QCD while the prediction for  $g_L$  is not

published. Moreover, most of the analysis frequently assume real values for  $g_R$  and  $g_L$ . The quantum corrections coming from the SM should be under known in order to discriminate the SM and new physics contributions from data.

Let us briefly review the experimental status for the constraints on these tensor couplings. Indirect limits on  $g_L$  and  $g_R$  can be obtained from  $b \rightarrow s\gamma$  in the measured branching ratio  $B(\bar{B} \rightarrow X_s\gamma)$ . The results from a recent analysis [18] are given in the first line of Table 1.

Table 1: Bounds on  $g_R$  and  $g_L$ . The first line shows the indirect limits from  $b \rightarrow s\gamma$ . The second and third lines are limits obtained from simulations for the LHC. The last two lines show  $3\sigma$  discovery limits intervals: fourth line limits are from simulations for the LHC and the last one is from  $b \rightarrow s\gamma$ .

Reference		$g_R$ bound	$g_L$ bound
[18]	95%C.L.	$-0.15 < g_R < 0.57$	$-0.0015 < g_L < 0.0004$
[12]	$2\sigma$	$-0.026 \leq g_R \leq 0.031$	$-0.058 \leq g_L \leq 0.026$
[6]	$1\sigma$	$-0.012 \leq g_R \leq 0.024$	$-0.16 \leq g_L \leq 0.16$
		$g_R$ discovery limit	$g_L$ discovery limit
[13]	$3\sigma$	$ Re(g_R)  \geq 0.056$	$Re(g_L) \geq 0.051$ or $Re(g_L) \leq -0.083$
		$ Im(g_R)  \geq 0.115$	$ Im(g_L)  \geq 0.065$
[13, 18]	$3\sigma$	$Re(g_R) \geq 0.76$ or $Re(g_R) \leq -0.33$	$Re(g_L) \geq 0.0009$ or $Re(g_L) \leq -0.0019$ $ Im(g_L)  \geq 0.006$

The constraints on  $g_L$  are much stronger than those on  $g_R$  due to the chiral  $m_t/m_b$  enhancement factor which comes together with the  $g_L$  coupling in the  $B$ -meson decay amplitude. These bounds are obtained assuming that all anomalous couplings are real and that only one of them is non zero at a time.

The top width  $\Gamma_t$  is an observable which is sensitive to the absolute strength of the  $tbW$  vertex but with no particular sensitivity to the anomalous couplings. Another test of the Lorentz structure of the  $tbW$  amplitude is the measurement of the polarized decay fractions  $Br(t \rightarrow bW_\lambda^+)$  into  $W^+$  bosons of helicity  $\lambda = 0, \mp 1$ . The SM values for this  $W$ -polarized widths are known up to one loop QCD and electroweak corrections [8] and the contribution to the helicity fractions from the anomalous couplings defined in Eq.[1] were computed in [9, 10]. However, these fractions are sensitive only to ratios of the couplings. Other observables can be obtained from the single top production at the LHC [6]. From a combined analysis of

the single top cross section and the three helicity fractions, the four anomalous couplings in Eq.[1] can be determined. Also,  $g_R$  could be measured from the energy and angular distributions for polarized semi-leptonic and hadronic top-quark decays as was studied in [19].

The Tevatron found no deviation from the SM in top quark physics. It has also investigated the anomalous couplings based on the single top quark production cross section [20]. These are the first direct experimental bounds but they are not competitive with the indirect ones already mentioned. In the near future the LHC high statistics data on top quark decays will allow the direct determination of the tensor couplings  $g_L$  and  $g_R$  within a few percent level. In particular, in simulations for  $t\bar{t}$  production and decay in dileptonic [21] and lepton plus jets channels [12, 19, 21], forward-backward asymmetries [12] and a double angular distribution in  $t$ -quark decay [19] were studied. In [12], with only one non standard coupling different from zero at a time, intervals for detection or exclusion at two standard deviations (both statistical and systematic uncertainties included) for  $g_L$  and  $g_R$  were predicted for the future LHC data; they are shown in the second line of Table 1. The LHC will possibly improve the sensitivity to  $g_R$  by an order of magnitude when compared to the indirect bounds from  $b \rightarrow s\gamma$ . A combined fit, using the four couplings  $V_L$ ,  $V_R$ ,  $g_R$  and  $g_L$  as parameters, and taking into account the expected uncertainties at the LHC for top-quark decay was presented in [6] and it is shown in the third line of Table 1. The sensitivity to  $g_R$  shown in the second and third lines of Table 1 is similar to the results of [19, 21] where  $t\bar{t}$  production and decay into leptonic and dileptonic decay channels were analyzed.

Recently, new helicity fractions of the W were defined and investigated for polarized top decays. The spin matrix for polarized top decays was obtained in [13]; they also considered new observables derived from the normal and transverse  $W^+$  polarization fractions. A similar approach in asymmetry observables was also studied in Tau physics in recent years [22]. The three different sets of W helicity fractions defined for the polarized top quark were shown to open the possibility of new observables particularly sensitives to both the real and imaginary parts of the tensor couplings. They compute the  $3\sigma$  discovery limits for  $g_R$  and  $g_L$  assuming that they are either real or purely imaginary and allowing only one coupling to be different from zero at a time. The exclusion intervals are shown in Table 1 in the fourth line. As a reference for the comparison of the potential of the LHC they also derived the  $3\sigma$  discovery limits from  $b \rightarrow s\gamma$  in [18]; this is shown in the last line of Table 1.

It is generally believed that beyond the SM theories will be probed in top quark physics. These theories, in general, not only will induce non zero values of  $g_R$  and  $g_L$  but also may be responsible for new exotic decay modes. The top dominant decay mode,  $t \rightarrow bW^+$ , was investigated in many extension of the SM. In particular, the decay rate and polarized decay

fractions were studied in many theories such as the Two Higgs Doublet Model (2HDM), the minimal supersymmetric SM (MSMM) and top-color assisted technicolor (TC2). These results were reviewed in [7] where some of the anomalous couplings were computed for these models. For the first two of them they found the general feature that  $|g_R| \gg |g_L|$  and  $|Re(g_R)| \gg |Im(g_L)|$ . Besides, they found that values of  $g_R$  up to  $0.5 \times 10^{-3}$  are possible for low  $\tan\beta$ , while only  $0.2 \times 10^{-3}$  is expected for higher values of  $\tan\beta$ . Notice that these two last figures represent 8% and 3%, respectively, of the leading one loop gluon contribution. For TC2 models they showed that values for  $g_R$  as big as 0.01 can be expected, and this represents 150% of the one loop gluon contribution. The general feature  $|g_R| \gg |g_L|$  and  $|Re(g_R)| \gg |Im(g_L)|$  is also true for the SM, as it will be shown in the following sections.

### 3 Electroweak corrections to the anomalous couplings $g_R$ and $g_L$

In the SM, at one loop, there is only one topology for the vertex correction diagrams that contribute to the anomalous  $g_R$  and  $g_L$  couplings. This is shown in Figure 1(a) and we will denote this diagram as ABC using the name of the particles circulating in the loop. The QCD one loop gluon contribution ( $ABC = gtb$ ) dominates the standard contribution in both the  $g_R$  and  $g_L$  dipole moments. All these diagrams, 19 as a whole, can be classified according to their dependence on the quark masses. As already mentioned, the tensorial

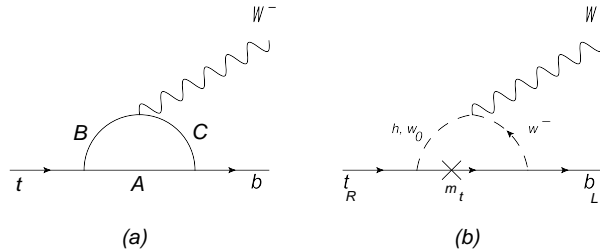


Figure 1: a. Topology of the one-loop SM Feynman diagrams for the quantum correction to the decay  $t \rightarrow bW^+$ . b. Leading order diagrams for  $g_R$  in the large  $m_t$  limit.

anomalous couplings we are interested in are chirality flipping magnitudes so, in general, a mass insertion is needed in order for the diagram to contribute. All contributions to  $g_R$  need a  $m_t$  mass insertion while the contributions to  $g_L$  need a  $m_b$  mass insertion. The different mass insertions for each diagram is shown in Figure 2. Besides, some of the vertex have also a mass dependence. For all these diagrams there are three mass dependencies that are different for the case of  $g_R$  and for  $g_L$ . We use this fact in order to classify all the contributions



coming from all the diagrams. For  $g_R$  there are two diagrams that have a leading  $m_t$ -mass

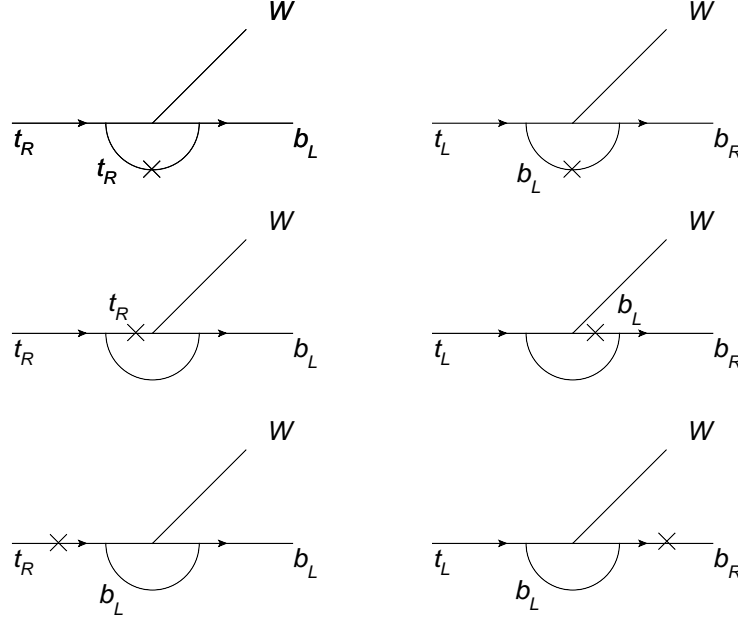


Figure 2: Mass insertions for the diagrams: in the left we can see the case for  $g_R$  where a factor  $m_t$  is present for each diagram while the ones at the right are for  $g_L$  and proportional to  $m_b$ .

dependence, with non-decoupling in the  $m_t$  mass [23]. They are the ones with  $thW$  and  $tw_0W$  circulating in the loop, where  $h$  is the Higgs boson and  $w_0$  is the unphysical Z-boson; they are shown in Figure 1(b). These two diagrams have top mass-insertions that, together with the mass coming from the vertex, finally gives a mass dependence that is of the order  $1/r_w^2$ , where  $r_w^2 = (m_W/m_t)^2$ , with respect to the other diagrams. Next, there are 12 diagrams that also have a top mass insertion but do not have this  $1/r_w^2$  enhancement factor; all of them have a similar mass dependence. The QCD gluon exchange diagram also needs a top mass insertion for  $g_R$ . The remaining four diagrams do not have the  $1/r_w^2$  enhancement factor but a suppression factor  $r_b^2 = (m_b/m_t)^2$  coming from the mass dependence of the vertex and from a b-quark mass insertion. The particles circulating in the loop for these diagrams are  $bw^+w_0$ ,  $bw^+h$ ,  $htb$  and  $w_0tb$ , where  $w^\pm$  are the unphysical W-bosons. All these last diagrams turn out to be numerically insignificant as the small  $r_b$  coefficient may suggest. Finally, the diagrams that dominate the final value for this electroweak correction are the ones of the first two classes we have already presented. In the computation we find that there is no numerical domination of the first ones with the  $m_t$  non-decoupling effect over the ones without this effect. The  $g_R$  coupling is finite and, up to one loop, the calculation needs no renormalization. However, not all the diagrams are infrared finite: some cancellation



occurs among some groups of them in such a way as to end up with a finite value. This fact was used as a check of our results. This is the case for the diagrams  $t\gamma W$  and  $tW\gamma$  and also for  $b\gamma W$  and  $bW\gamma$ . There are no singularities when we sum each pair together for the computation. Some diagrams, like  $bWZ$  for example, contribute to the imaginary part of  $g_R$ . In these cases we also used the Cutkosky rules and compared the result with the direct computation as a double check of our numerical calculation. Besides, some of the integrals can be done analytically up to the end and we verified the numerical evaluation of these results with the numerical evaluation of the Feynman integrals. This check was possible for the diagrams with a gluon or a photon circulating in the loop. All these facts allow for a multiple check of our calculations. As already anticipated, we can read in Table 2 that the value of the four diagrams with the  $r_b^2$  factor are numerical negligible. Each diagram

Table 2: Electroweak contributions to  $g_R$  and  $g_L$ .

Diagram	$g_R \times 10^3$	$g_L \times 10^3$
$tZW$	-1.176	-0.0141
$thW$	0.220	0
$tw^0w^-$	0.344	0.0051
$thw^-$	0.462	-0.0088
$tZw^-$	-0.050	-0.0012
$t\gamma W + t\gamma w^-$	0.572	-0.0094
$bWZ$	$-0.623 - 0.664i$	$-0.0201 - 0.0214i$
$bWh$	0	$0.0086 - 0.0120i$
$bw^+w^0$	$(1.5 + 11.0i) \times 10^{-4}$	$-0.0029 - 0.0167i$
$bw^+h$	$(-4.3 + 8.6i) \times 10^{-4}$	$-0.0019 + 0.0111i$
$bw^+Z$	$-0.088 - 0.062i$	$-0.00039 - 0.00028i$
$bW\gamma + bw^+\gamma$	$0.114 - 0.509i$	$-0.0270 + 0.0250i$
$Ztb$	-0.397	-0.0067
$\gamma tb$	0.068	0.0115
$w^0tb$	$-6.8 \times 10^{-4}$	-0.0109
$htb$	$-6.2 \times 10^{-4}$	-0.0135
$\Sigma(EW)$	$-0.56 - 1.23i$	$-(0.092 + 0.014i)$
g t b	-6.61	-1.12
Total	$-7.17 - 1.23i$	$-1.212 - 0.014i$

contributes with a different sign to the final result so finally many of them are numerically

responsible for the final numerical value that can not be anticipated without an explicit and careful computation of all of them. The figures for each contribution of the diagrams to  $g_R$  and  $g_L$  is given in Table 2, where we take the Higgs mass value  $m_h = 150$  GeV. We can read in the Appendix A the expressions for each of the diagrams as well as the analytical results (Appendix B) for some of the diagrams for which it was feasible. We also show, in Appendix B, the limit  $m_b \rightarrow 0$  for these last formulas. This was also used as a check of our numerical evaluation of the integrals. The results are rather insensitive to the Higgs mass value in the experimental allowed Higgs mass interval [16]. The final result for the one loop electroweak correction for the magnetic right anomalous coupling is:

$$g_R^{EW} = -(0.56 + 1.23i) \times 10^{-3}. \quad (2)$$

Note that we have real and imaginary parts in this dipole moment and that the last is more than double of the first. These values are to be compared with the gluon contribution that is the dominant one:

$$g_R^g = -6.61 \times 10^{-3}. \quad (3)$$

This last result agrees with the one given in reference [15] if we put the numerical values for masses and couplings used at that time. The final result for the one loop computation in the SM is the sum of the last two values given in Eqs.[2] and [3]:

$$g_R^{SM} = -(7.17 + 1.23i) \times 10^{-3}. \quad (4)$$

The real part for the one loop electroweak quantum correction for  $g_R$  is 8% of the leading gluon-exchange contribution. The CP-even imaginary absorptive part, generated by electroweak corrections, may be measured with a similar set of observables as those considered in the literature to measure  $g_R$  and, more specifically,  $Re(g_R)$ . Note that this imaginary part is 17% of the one loop  $Re(g_R^{SM})$ .

The one loop electroweak correction for the  $g_L$  coupling can be obtained in a similar way as in the previous calculation, however a b-quark mass insertion is present in all the diagrams because  $g_L$  couples to a right b-quark. This factor dominates the numerical value of the final result for the  $g_L$  electroweak contributions. As in the previous computation, there are also IR divergences in the same diagrams as in the preceding calculation and again they sum up to a finite result. The same checks we already explained before for  $g_R$  have been used. We also find that an imaginary part for the electroweak contribution to  $g_L$  shows up, so the final result is:

$$g_L^{EW} = -(0.92 + 0.14i) \times 10^{-4}. \quad (5)$$

This is to be compared and summed with the gluon contribution, that is real and the dominant one, in order to obtain the one loop result:

$$g_L^g = -1.12 \times 10^{-3}. \quad (6)$$

The final result for the one loop computation in the SM is then:

$$g_L^{SM} = -(1.21 + 0.01i) \times 10^{-3}. \quad (7)$$

We note that for  $g_L$  the electroweak contribution is again 8% of the gluon contribution for  $g_L$ , and the CP-even imaginary part has its origin in the electroweak diagrams.

## 4 Conclusions

We have computed the one loop electroweak values of the anomalous form factors  $g_R$  and  $g_L$  for the decay  $t \rightarrow bW^+$ . Both of them have real and imaginary parts. The imaginary parts come from the electroweak correction and, for  $g_R$ , it is almost three times the real part, while for  $g_L$ , it is 15% of the real one. Contrary to what happens in extended models, where the imaginary part are usually negligible if the new particles involved have higher mass scale than the top, we found that the absorptive parts of the dipole moments, which are induced in the SM by  $CP$ -invariant final-state re-scattering, has to be taken into account and may have physical effects that could be detected in the future through the observables proposed in the literature. Note that the  $g_R$  coupling will be measured at the LHC and its absorptive contribution may be accessible in data and in the new observables defined in [13], for example. For the SM one loop  $g_R$  coupling, the imaginary part is about 17% of the real one while, for  $g_L$ , it is only 1%. The value of the  $g_L$  dipole moment, although proportional to  $m_b$ , is only about one order of magnitude smaller than  $g_R$ . The SM prediction for the real part of  $g_L$  is  $Re(g_L) \simeq -0.0012$  and is very close to the estimated  $3\sigma$  indirect discovery limit,  $Re(g_L) \leq -0.0019$ , obtained from  $b \rightarrow s\gamma$  in [13] based on the results of [18], so any contribution coming from new physics that may show up may be in conflict with these bounds. Besides, the value of the electroweak corrections for these dipole moments, first published in this paper can, by themselves, explain deviations up to a few percent level in the observables, that are frequently discussed in the literature in connection to extended models.

## Acknowledgments

This work was supported in part by Pedeciba and CSIC - Uruguay, by COLCIENCIAS - Colombia, by the Spanish Ministry of Science and Innovation (MICINN), under grants FPA2008-03373, FPA2008-02878, and by Generalitat Valenciana under grant PROMETEO 2009/128. G.A.G.S. also thanks the Universitat de Valencia for the hospitality and support during his stay at the Theoretical Physics Department.

## A Expressions for the diagrams

For the  $g_R$  and  $g_L$  couplings the contribution coming from each of the diagrams are written with the help of the following denominators:

$$\begin{aligned}
A_Z &= x^2 \left( ((y-1)r_b^2 + 1)y - r_w^2(y-1) \right) - r_z^2(x-1) \\
B_Z &= x \left( ((x(y-1) + 1)r_b^2 + x - 1)y - r_z^2(y-1) \right) - r_w^2(x-1)(x(y-1) + 1) \\
C_Z &= (x-1)(xy-1)r_b^2 - r_w^2(x-1)x(y-1) + r_z^2xy + x(y-1)(xy-1) \\
\{A_\gamma, B_\gamma, C_\gamma\} &= \{A_Z, B_Z, C_Z\} (r_z \rightarrow 0) \\
\{A_H, B_H, C_H\} &= \{A_Z, B_Z, C_Z\} (r_z \rightarrow r_h)
\end{aligned}$$

The contribution of each diagram to  $g_L$  is:

$$\begin{aligned}
g_L^{tZW} &= \frac{e^2 V_{tb}^* r_w r_b}{128 \pi^2 s_w^2} \times \int_0^1 dx \int_0^1 dy \frac{-2(a_t + v_t)x(2(y-1)yx^2 - 2yx + x + 1)}{A_Z} \\
g_L^{t\gamma W} &= \frac{e^2 Q_t V_{tb}^* r_w r_b}{32 \pi^2} \times \int_0^1 dx \int_0^1 dy \frac{-2x(2(y-1)yx^2 - 2yx + x + 1)}{A_\gamma} \\
g_L^{thW} &= 0 \\
g_L^{tw_0 w^-} &= -\frac{e^2 V_{tb}^* r_b}{128 \pi^2 r_w s_w^2} \times \int_0^1 dx \int_0^1 dy \frac{-2x^3 y^2}{A_Z} \\
g_L^{thw^-} &= -\frac{e^2 V_{tb}^* r_b}{128 \pi^2 r_w s_w^2} \times \int_0^1 dx \int_0^1 dy \frac{2x^2(x(y-2) + 2)y}{A_H} \\
g_L^{tZw^-} &= \frac{e^2 V_{tb}^* r_w r_b}{128 c_w^2 \pi^2} \times \int_0^1 dx \int_0^1 dy \frac{2(a_t + v_t)(x-1)x}{A_Z} \\
g_L^{t\gamma w^-} &= -\frac{e^2 Q_t V_{tb}^* r_w r_b}{32 \pi^2} \times \int_0^1 dx \int_0^1 dy \frac{2x(x-1)}{A_\gamma} \\
g_L^{bWZ} &= \frac{e^2 V_{tb}^* r_w r_b}{128 \pi^2 s_w} \times \int_0^1 dx \int_0^1 dy \frac{2x}{B_Z} \left[ a_b(2(y-1)yx^2 - 5yx + x + 4) + \right. \\
&\quad \left. v_b(2(y-1)yx^2 + (y+1)x - 2) \right]
\end{aligned}$$

$$\begin{aligned}
g_L^{bW\gamma} &= \frac{e^2 Q_b V_{tb}^* r_w r_b}{32\pi^2} \times \int_0^1 dx \int_0^1 dy \frac{2x(2(y-1)yx^2 + (y+1)x - 2)}{B_\gamma} \\
g_L^{bWh} &= \frac{e^2 V_{tb}^* r_w r_b}{64\pi^2 s_w^2} \times \int_0^1 dx \int_0^1 dy \frac{-2(x-1)x}{B_H} \\
g_L^{bw^+w_0} &= -\frac{e^2 V_{tb}^* r_b}{128\pi^2 r_w s_w^2} \times \int_0^1 dx \int_0^1 dy \frac{2x^2((x(y-1)+1)r_b^2 + x - 1)y}{B_Z} \\
g_L^{bw^+h} &= -\frac{e^2 V_{tb}^* r_b}{128\pi^2 r_w s_w^2} \times \int_0^1 dx \int_0^1 dy \frac{2x^2((x(y-1)-1)r_b^2 - x + 1)y}{B_H} \\
g_L^{bw^+Z} &= \frac{e^2 V_{tb}^* c_w r_w r_b}{128c_w^2 \pi^2} \times \int_0^1 dx \int_0^1 dy \frac{-2(a_b - v_b)x^2(y-1)}{B_Z} \\
g_L^{bw^+\gamma} &= -\frac{e^2 Q_b V_{tb}^* r_w r_b}{32\pi^2} \times \int_0^1 dx \int_0^1 dy \frac{2x^2(y-1)}{B_\gamma} \\
g_L^{Ztb} &= -\frac{e^2 V_{tb}^* r_w r_b}{512\pi^2 c_w^2 s_w^2} \times \int_0^1 dx \int_0^1 dy \frac{-4(a_t + v_t)x^2 y}{C_Z} [v_b(x-1) + a_b(x+1)] \\
g_L^{\gamma tb} &= -\frac{e^2 Q_b Q_t V_{tb}^* r_w r_b}{32\pi^2} \times \int_0^1 dx \int_0^1 dy \frac{-4(x-1)x^2 y}{C_\gamma} \\
g_L^{w_0 tb} &= \frac{e^2 V_{tb}^* r_b}{128\pi^2 r_w s_w^2} \times \int_0^1 dx \int_0^1 dy \frac{-2x^2(y-1)(xy-1)}{C_Z} \\
g_L^{htb} &= \frac{e^2 V_{tb}^* r_b}{128\pi^2 r_w s_w^3} \times \int_0^1 dx \int_0^1 dy \frac{2x^2(y-1)(xy+1)}{C_H}
\end{aligned}$$

while for  $g_R$  we have:

$$\begin{aligned}
g_R^{tZW} &= \frac{e^2 V_{tb}^* r_w}{128\pi^2 s_w^2} \times \\
&\quad \int_0^1 dx \int_0^1 dy \frac{2x(v_t(-2yx^2 + x + 1) + a_t(-2yx^2 + 6yx + x - 5))}{A_Z} \\
g_R^{t\gamma W} &= \frac{e^2 Q_t V_{tb}^* r_w}{32\pi^2} \times \int_0^1 dx \int_0^1 dy \frac{2x(-2yx^2 + x + 1)}{A_\gamma} \\
g_R^{thW} &= \frac{e^2 V_{tb}^* r_w}{64\pi^2 s_w^2} \times \int_0^1 dx \int_0^1 dy \frac{2x^2(1-y)}{A_H} \\
g_R^{tw_0 w^-} &= -\frac{e^2 V_{tb}^*}{128\pi^2 r_w s_w^2} \times \int_0^1 dx \int_0^1 dy \frac{2x^3(-(y-1)r_b^2 - 1)y}{A_Z} \\
g_R^{thw^-} &= -\frac{e^2 V_{tb}^*}{128\pi^2 r_w s_w^2} \times \int_0^1 dx \int_0^1 dy \frac{2x^2(x(1-r_b^2(y-1)) - 2)y}{A_H} \\
g_R^{tZw^-} &= \frac{e^2 V_{tb}^* r_w}{128c_w^2 \pi^2} \times \int_0^1 dx \int_0^1 dy \frac{2(a_t - v_t)(x-1)x}{A_Z} \\
g_R^{t\gamma w^-} &= -\frac{e^2 Q_t V_{tb}^* r_w}{32\pi^2} \times \int_0^1 dx \int_0^1 dy \frac{-2x(x-1)}{A_\gamma} \quad (\text{diverge})
\end{aligned}$$

$$\begin{aligned}
g_R^{bWZ} &= \frac{e^2 V_{tb}^* r_w}{128\pi^2 s_w} \times \int_0^1 dx \int_0^1 dy \frac{2(a_b + v_b)x(2yx^2 - (3y+1)x + 2)}{B_Z} \\
g_R^{bW\gamma} &= \frac{e^2 Q_b V_{tb}^* r_w}{32\pi^2} \times \int_0^1 dx \int_0^1 dy \frac{2x(2yx^2 - (3y+1)x + 2)}{B_\gamma} \\
g_R^{bWh} &= \frac{e^2 r_b V_{tb}^* r_w}{64\pi^2 s_w^2} \times 0 = 0 \\
g_R^{bw^+w_0} &= -\frac{e^2 r_b V_{tb}^*}{128\pi^2 r_w s_w^2} \times \int_0^1 dx \int_0^1 dy \frac{2r_b x^3 y^2}{B_Z} \\
g_R^{bw^+h} &= -\frac{e^2 r_b V_{tb}^* r_w}{128\pi^2 r_w^2 s_w^2} \times \int_0^1 dx \int_0^1 dy \frac{-2r_b x^3 (y-2)y}{B_H} \\
g_R^{bw^+Z} &= \frac{e^2 V_{tb}^* s_w r_w}{128c_w^2 \pi^2} \times \int_0^1 dx \int_0^1 dy \frac{-2(a_b + v_b)x^2(y-1)}{B_Z} \\
g_R^{bw^+\gamma} &= -\frac{e^2 Q_b V_{tb}^* r_w}{32\pi^2} \times \int_0^1 dx \int_0^1 dy \frac{-2x^2(y-1)}{B_\gamma} \\
g_R^{Ztb} &= -\frac{e^2 V_{tb}^* r_w}{512c_w^2 \pi^2 s_w^2} \times \\
&\quad \int_0^1 dx \int_0^1 dy \frac{-4(a_b + v_b)x^2(a_t(x(y-1) + 2) + v_t x(y-1))y}{C_Z} \\
g_R^{\gamma tb} &= -\frac{e^2 Q_b Q_t V_{tb}^* r_w}{32\pi^2} \times \int_0^1 dx \int_0^1 dy \frac{-4x^3(y-1)y}{C_\gamma} \\
g_R^{w_0 tb} &= \frac{e^2 V_{tb}^* r_b}{128\pi^2 r_w s_w^2} \times \int_0^1 dx \int_0^1 dy \frac{-2r_b(x-1)x(xy-1)}{C_Z} \\
g_R^{htb} &= \frac{e^2 V_{tb}^* r_b}{128\pi^2 r_w s_w^2} \times \int_0^1 dx \int_0^1 dy \frac{2r_b(x-1)x(xy+1)}{C_H}
\end{aligned}$$

## B Some exact results

The following integrals, corresponding to diagrams with a photon or gluon circulating in the loop,  $t\gamma W$ ,  $t\gamma w^-$ ,  $bW\gamma$ ,  $bw^+\gamma$ ,  $\gamma tb$  and  $gtb$ , can be done analytically. Using the notation

$$g_{L,R}^{ABC} = \frac{e^2 V_{tb}^* r_w}{32\pi^2} Q \times I_{L,R}^{ABC}$$

we have:

$$\begin{aligned}
I_R^{t\gamma W + t\gamma w^-} &= \frac{4}{\Delta} \left[ \left( \left( 1 + \frac{1 - r_w^2 - r_b^2 + \Delta}{4r_b^2} \right) \log \left( \frac{1 - r_w^2 + r_b^2 + \Delta}{1 - r_w^2 - r_b^2 + \Delta} \right) \right) - \left( \Delta \rightarrow -\Delta \right) \right] \\
I_L^{t\gamma W + t\gamma w^-} &= \frac{2}{r_b} \left[ 1 - \left( \frac{(1 - r_w^2 + r_b^2 + \Delta)(1 - r_w^2 + 3r_b^2 + \Delta)}{4r_b^2 \Delta} \log \left( \frac{1 - r_w^2 + r_b^2 + \Delta}{1 - r_w^2 - r_b^2 + \Delta} \right) \right) \right. \\
&\quad \left. - \left( \Delta \rightarrow -\Delta \right) \right]
\end{aligned}$$

$$\begin{aligned}
I_R^{tW\gamma+tw^+\gamma} &= -\frac{2i\pi}{\Delta} [2 - 3r_w^2 + r_w^4 + r_b^4 + r_b^2(1 - 2r_w^2)] - 2 + 2(2 - r_w^2 + r_b^2) \log(2r_b^2) + \\
&\quad \frac{4r_b^2}{\Delta} \left[ \left( \frac{1 - r_w^2 + 3r_b^2 + \Delta}{(1 - r_w^2 + r_b^2 + \Delta)^2} \log(1 - r_w^2 - r_b^2 + \Delta) \right) - (\Delta \rightarrow -\Delta) \right] \\
I_L^{tW\gamma+tw^+\gamma} &= \frac{2r_b}{\Delta} \left[ \left( \frac{1 - r_w^2 + 3r_b^2 + \Delta}{1 - r_w^2 + r_b^2 + \Delta} \log(1 - r_w^2 - r_b^2 + \Delta) \right) - (\Delta \rightarrow -\Delta) \right] - \\
&\quad 2r_b \log(2r_b^2) + \frac{2i\pi r_b}{\Delta} (3 - r_w^2 + r_b^2) \\
I_R^{\eta b} &= \frac{2}{\Delta} \left[ \left( \frac{1 - r_w^2 + r_b^2 + \Delta}{1 + r_w^2 - r_b^2 - \Delta} \log \left( \frac{2}{1 - r_w^2 + r_b^2 + \Delta} \right) \right) - (\Delta \rightarrow -\Delta) \right] \\
I_L^{\eta b} &= \frac{4r_b}{\Delta} \left[ \left( \frac{1}{1 + r_w^2 - r_b^2 + \Delta} \log \left( \frac{2}{1 - r_w^2 + r_b^2 - \Delta} \right) \right) - (\Delta \rightarrow -\Delta) \right]
\end{aligned}$$

with  $\Delta = \sqrt{1 - 2(r_w^2 + r_b^2) + (r_b^2 - r_w^2)^2}$ . These expressions can be written, in the  $m_b \rightarrow 0$  limit, as:

$$\begin{aligned}
I_R^{tW\gamma+tw^-\gamma} &\approx \frac{2}{1 - r_w^2} \left[ 1 + \frac{(2 - r_w^2)}{1 - r_w^2} \log(r_w^2) \right] + \\
&\quad \frac{r_b^2}{(1 - r_w^2)^4} [3(r_w^4 - 4r_w^2 + 3) + 2(2 + 2r_w^2 - r_w^4) \log(r_w^2)] + O(r_b^4) \\
I_L^{tW\gamma+tw^-\gamma} &\approx \frac{r_b}{(1 - r_w^2)^3} [8r_w^2 - 3r_w^4 - 5 + 2(r_w^2 - 2) \log(r_w^2)] + \\
&\quad \frac{4r_b^3}{3(1 - r_w^2)^5} [9r_w^2 - r_w^6 - 8 + 3(r_w^4 - 2r_w^2 - 1) \log(r_w^2)] + O(r_b^5) \\
I_R^{tW\gamma+tw^+\gamma} &\approx -2i\pi \left[ 2 - r_w^2 + \frac{r_b^2}{(1 - r_w^2)^2} (3 - 2r_w^2 + r_w^4) \right] - 2 \left[ 1 + (2 - r_w^2) \log \frac{r_w^2}{1 - r_w^2} \right] - \\
&\quad \frac{2r_b^2}{(1 - r_w^2)^2} [\log(r_b^2) - (3 - 2r_w^2 + r_w^4) \log(1 - r_w^2) + (2 - 2r_w^2 + r_w^4) \log(r_w^2)] + \\
&\quad O(r_b^4) \\
I_L^{tW\gamma+tw^+\gamma} &\approx 2i\pi \frac{r_b}{1 - r_w^2} \left( 3 - r_w^2 + \frac{4r_b^2}{(1 - r_w^2)^2} \right) + \\
&\quad \frac{2r_b}{1 - r_w^2} [\log(r_b^2) + (2 - r_w^2) \log(r_w^2) - (3 - r_w^2) \log(1 - r_w^2)] - \\
&\quad \frac{2r_b^3}{(1 - r_w^2)^3} [1 + 2 \log(r_b^2) + 2 \log(r_w^2) - 4 \log(1 - r_w^2)] + O(r_b^5) \\
I_R^{\eta b} &\approx -\frac{2}{r_w^2} \log(1 - r_w^2) + \frac{2r_b^2}{(1 - r_w^2)^2} [1 + \log(r_b^2) - 2 \log(1 - r_w^2)] + O(r_b^4) \\
I_L^{\eta b} &\approx \frac{-2r_b}{1 - r_w^2} \left[ \log(r_b^2) - \frac{1 + r_w^2}{r_w^2} \log(1 - r_w^2) \right] - \\
&\quad \frac{2r_b^3}{(1 - r_w^2)^3} [1 + 2 \log(r_b^2) - 4 \log(1 - r_w^2)] + O(r_b^5)
\end{aligned}$$



## References

- [1] E. W. Varnes [CDF and D0 Collaborations], *Int.J.Mod.Phys. A* **23** (2008) 4421.
- [2] M. Beneke *et al.*, hep-ph/0003033.
- [3] W. Bernreuther, *J. Phys. G* **G35** (2008) 083001; E. Boos, L. Dudko and T. Ohl, *Eur. Phys J. C* **11** (1999) 473.
- [4] C.E. Gerber *et al.*, [TeV4LHC-Top and Electroweak Working Group], hep-ph/0705.3251.
- [5] C.J.C. Burges and H.J.Schnitzer, *Nucl. Phys. B* **228** (1983) 454; C.N. Leung, S.T. Love and S. Rao, *Z. Phys C* **31** (1986) 433; W. Buchmuller and D. Wyler, *nucl. Phys. B* **268** (1986) 621.
- [6] J. A. Aguilar-Saavedra, *Nucl. Phys. B* **804** (2008) 160.
- [7] W. Bernreuther, P. González and M. Wiebusch, *Eur. Phys. J.C* **60** (2009) 197.
- [8] H.S. Do, S. Groote, J.G. Korner, M.C. Mauser, *Phys. Rev. D* **67** (2003) 091501.
- [9] C.R. Chen, F. Larios, C.P. Yuan, *Phys. Lett. B* **631** (2005) 126.
- [10] J. A. Aguilar-Saavedra, J. Carvalho, N. Castro, F. Veloso and A. Onofre, *Eur. Phys. J. C* **50** (2007) 519.
- [11] F. del Águila and J.A. Aguilar-Saavedra, *Phys. Rev. D* **67** (2003) 014009.
- [12] J. A. Aguilar-Saavedra, J. Carvalho, N. Castro, A. Onofre and F. Veloso, *Eur. Phys. J. C* **53** (2008) 689.
- [13] J. Bernabéu and J.A. Aguilar-Saavedra, *Nucl. Phys. B* **840** (2010) 349.
- [14] M. Jezabek and J. H. Kuhn, *Phys. Rev. D* **48** (1993) 1910 [Erratum-ibid. *D* **49** (1994) 4970]; A. Czarnecki, *Phys. Lett. B* **252** (1990) 467.
- [15] C.S. Li, R.J. Oakes and T.C. Yuan, *Phys. Rev. D* **43** (1991) 3759.
- [16] K. Nakamura et al. (Particle Data Group), *J. Phys. G* **37** (2010) 075021.
- [17] J. Alwall *et al.*, *Eur. Phys. J. C* **49** (2007) 791.
- [18] B. Grzadkowski and M. Misiak, *Phys. Rev. D* **78** (2008) 077501.

- [19] S. Tsuno, I. Nakano, Y. Sumino and R. Tanaka, Phys. Rev. D **73** (2006) 054011.
- [20] V. M. Abazov *et al.* [D0 Collaboration], Phys. Rev. Lett. **101** (2008) 221801; Phys. Rev. Lett. **102** (2009) 092002.
- [21] F. Hubaut, E. Monnier, P. Pralavorio, K. Smolek and V. Simak, Eur. Phys. J. C **44 S2** (2005) 13.
- [22] J. Bernabéu, G.A. González-Sprinberg and J. Vidal, Phys. Lett. B **326** (1994) 168; J. Bernabéu, G.A. González-Sprinberg, M. Tung and J. Vidal, Nucl. Phys. B **436** (1995) 474.
- [23] J. Bernabéu, A. Pich and A. Santamaria, Phys. Lett. B **200** (1988) 569.